MYCOBIOLOGY
2026, VOL. 54, NO. 1, 120–132
https://doi.org/10.1080/12298093.2025.2610589

RESEARCH ARTICLE

OPEN ACCESS Check for updates

Unveiling Phyllosphere Fungal Communities in *Phytophthora infestans*-Infected Potatoes Through ITS Amplicon and FTIR Approaches in the Indonesian Highlands

Abdul Latief Abadi[a], Muhammad Akhid Syib'li[a], Irisa Trianti[a], Valia Istifada[b], Sholikah Widyanitta Rachmawati[b] and Bayu Aji Pamungkas[b]

[a]Department of Plant Pest and Disease, Faculty of Agriculture, Universitas Brawijaya, Malang, Indonesia; [b]Graduate Plant Pathology Study Program, Faculty of Agriculture, Universitas Brawijaya, Malang, Indonesia

ABSTRACT

Highland potato areas in East Java, Indonesia—Sumber Brantas and Tosari—face severe late blight caused by *Phytophthora infestans*. We profiled phyllosphere fungal communities (phylloplane plus leaf endosphere) on symptomatic potato leaves and examined how management contexts may relate to these assemblages. Leaves from "Granola Lembang" (Sumber Brantas) and "Granola Kembang" (Tosari) were analyzed using ITS amplicon sequencing (Nanopore) and Fourier-transform infrared (FTIR) spectroscopy. After normalization to relative abundances, α-diversity (Observed OTUs, Chao1, Shannon, Simpson) was higher in Tosari; communities were dominated by Ascomycota (putative endophytes/saprotrophs), whereas Sumber Brantas showed lower overall diversity with higher Mucoromycota. PCA of FTIR spectra separated samples by site, consistent with cross-site biochemical differences; however, we do not infer that FTIR differences are caused by community composition, nor that management variables are causal drivers. Instead, we treat management as contextual information that co-occurs with site, cultivar, and environmental/soil differences. Causal inference is not warranted given the two-site observational design, symptomatic-leaf sampling, different cultivars, and limited replication. Within these constraints, our integrative profiling provides hypothesis-generating baselines and suggests that management compatible with reduced chemical inputs may be associated with richer phyllosphere assemblages of potential biocontrol relevance in Indonesian highlands.

ARTICLE HISTORY
Received 28 August 2025
Revised 11 December 2025
Accepted 23 December 2025

KEYWORDS
Phytophthora infestans; phyllosphere; fungal diversity; FTIR

1. Introduction

Sumber Brantas and Tosari in East Java are among Indonesia's most important potato-producing regions. Sumber Brantas receives 1,785–2,447 mm annual rainfall, with average temperatures of 18–24 °C at 1,400–1,700 masl; Tosari receives ~2,101 mm, with cooler temperatures of 16–21 °C around 1,700 masl. Their cool climate and fertile volcanic soils provide conditions conducive to potato cultivation [1,2]. However, production faces substantial pressure from plant pathogens, notably *Phytophthora infestans*, the agent of late blight affecting foliage and tubers [3], with global annual losses exceeding US$6.7 billion [4]. In Indonesia, outbreaks in Tosari can cause losses up to 50%, whereas Sumber Brantas typically experiences ~30% yield reductions, with occasional crop failure.

P. infestans spreads rapidly under cool, humid conditions and can devastate crops within a short period [5,6]. Beyond yield loss, its persistence threatens farmer livelihoods and often increases reliance on fungicides [7]. Fungicides are widely used in Sumber Brantas and Tosari as primary control. While effective, repeated applications can perturb plant-surface and soil microbiota, with documented effects on bacterial and fungal community structures [8]. The phyllosphere—here defined to include both the phylloplane and the leaf endosphere—harbors diverse microbial communities that can contribute to disease suppression or facilitation [9]. In other crops (e.g., sorghum, cacao), phyllosphere fungal diversity has been associated with plant health outcomes [10,11], and genera such as *Trichoderma* antagonize pathogens *via* cell-wall-degrading enzymes [12]. Conversely, intensive fungicide use has been reported to reduce beneficial fungi and alter community composition [13,14].

Beyond chemical control, cultivation practices such as mulching and organic fertilization may modulate microbial dynamics. Mulching can improve soil health and support beneficial microbes [15,16],

CONTACT Muhammad Akhid Syib'li muhammad.syibli@ub.ac.id
Supplemental data for this article can be accessed online at https://doi.org/10.1080/12298093.2025.2610589.

whereas intensive fungicide regimes without such practices may coincide with lower diversity. In Sumber Brantas, fungicides including mancozeb, chlorothalonil, ametoctradin, and dimethomorph are routinely applied, whereas farmers in Tosari generally report less intensive chemical use with greater reliance on mulching and organic inputs. These contrasting contexts provide an opportunity to examine how agricultural practices may relate to phyllosphere fungal diversity [17].

Although shifts in soil microbiota under fungicide exposure and management have been documented [13,14], comparatively less is known about the potato phyllosphere under tropical highland conditions. Moreover, while amplicon-based (ITS) sequencing provides taxonomic resolution, its integration with biochemical approaches is limited. Fourier-transform infrared (FTIR) spectroscopy can capture biochemical residues and microbial metabolites [18–20]; in this study, its integration with sequencing-based community profiling is exploratory.

To address this gap, we profiled phyllosphere fungal communities on late-blight–symptomatic potato leaves from Sumber Brantas and Tosari using Oxford Nanopore ITS amplicon sequencing together with FTIR spectroscopy. Our goals are to describe cross-site patterns in community composition and biochemical profiles and to explore how these patterns co-occur with reported management practices. The study focuses on symptomatic leaves; healthy-leaf controls were not included and are identified as a priority for future controlled work. Given the two-site observational design, differences in cultivars and environmental/soil contexts, and limited replication, we do not make causal inferences; instead, we provide hypothesis-generating insights to inform microbiome-aware strategies for sustainable disease management.

2. Materials and methods

2.1. Study area and sampling

Samples were collected from two highland potato locations in East Java, Indonesia: Sumber Brantas Village, Batu City, and Tosari Village, Pasuruan Regency. GPS coordinates (decimal degrees) were recorded as Sumber Brantas (−7.761385, 112.529880) and Tosari (−7.876000, 112.894000) (Figure 1). Sumber Brantas is situated at 1,400–1,700 masl, with 1,785–2,447 mm annual rainfall and average temperatures of 18–24 °C. Tosari lies at ~1,700 masl, with ~2,101 mm annual rainfall and average temperatures of 16–21 °C. Both areas have fertile volcanic soils conducive to intensive potato cultivation [1,2]. The cultivated varieties differed by site: "Granola Lembang" in Sumber Brantas and "Granola Kembang" in Tosari.

At each location, five potato plants exhibiting typical late blight symptoms attributable to *Phytophthora infestans* were purposively selected. Plants were at a comparable growth stage (~40 days after planting, DAP). From each plant, one fully expanded mid-canopy symptomatic leaflet was sampled, yielding $n = 5$ leaves per site (ten leaves in total). Sampling was conducted during the dry season at ~18–20 °C and ~80% relative humidity. No surface sterilization was applied prior to DNA extraction; thus, in this study the phyllosphere profile includes both the phylloplane and the leaf endosphere. To obtain a site-level composite for sequencing, equal-mass aliquots from the five leaves per site were pooled into one composite DNA sample per site. Field blanks and extraction negative controls (NTCs) were included and processed alongside samples.

2.2. Microscopic examination of late-blight–symptomatic potato leaves

Microscopic observations were conducted on potato leaves showing characteristic symptoms of late blight. From each plant, the apical and marginal regions of symptomatic leaflets were selected as observation areas, focusing on the abaxial (lower) surface where sporulation typically occurs. Leaf pieces approximately 5 × 5 mm in size were placed abaxial-side down directly onto glass slides and examined under a bright-field light microscope using the dry-mount method (without mounting medium) to preserve the natural arrangement of surface structures.

To further resolve diagnostic morphology attributable to *Phytophthora infestans*, a complementary wet-mount preparation was made from the same symptomatic leaves by gently teasing mycelium from lesion margins with a sterile needle/forceps. The mycelium-bearing tissue was placed on a glass slide with a drop of sterile distilled water as the mounting medium, covered with a coverslip to avoid excessive compression, and examined under bright-field microscopy (400×) to visualize branched sporangiophores and ovoid to lemon-shaped sporangia.

Observations were performed using an Olympus BX41 microscope equipped with a digital camera Olympus DP26. Images were captured with the attached acquisition software under identical exposure settings; only linear adjustments to brightness and contrast were applied, with no image manipulation. The combined dry-mount and wet-mount procedures enabled visualization of surface-borne sporulation on naturally infected tissues while also

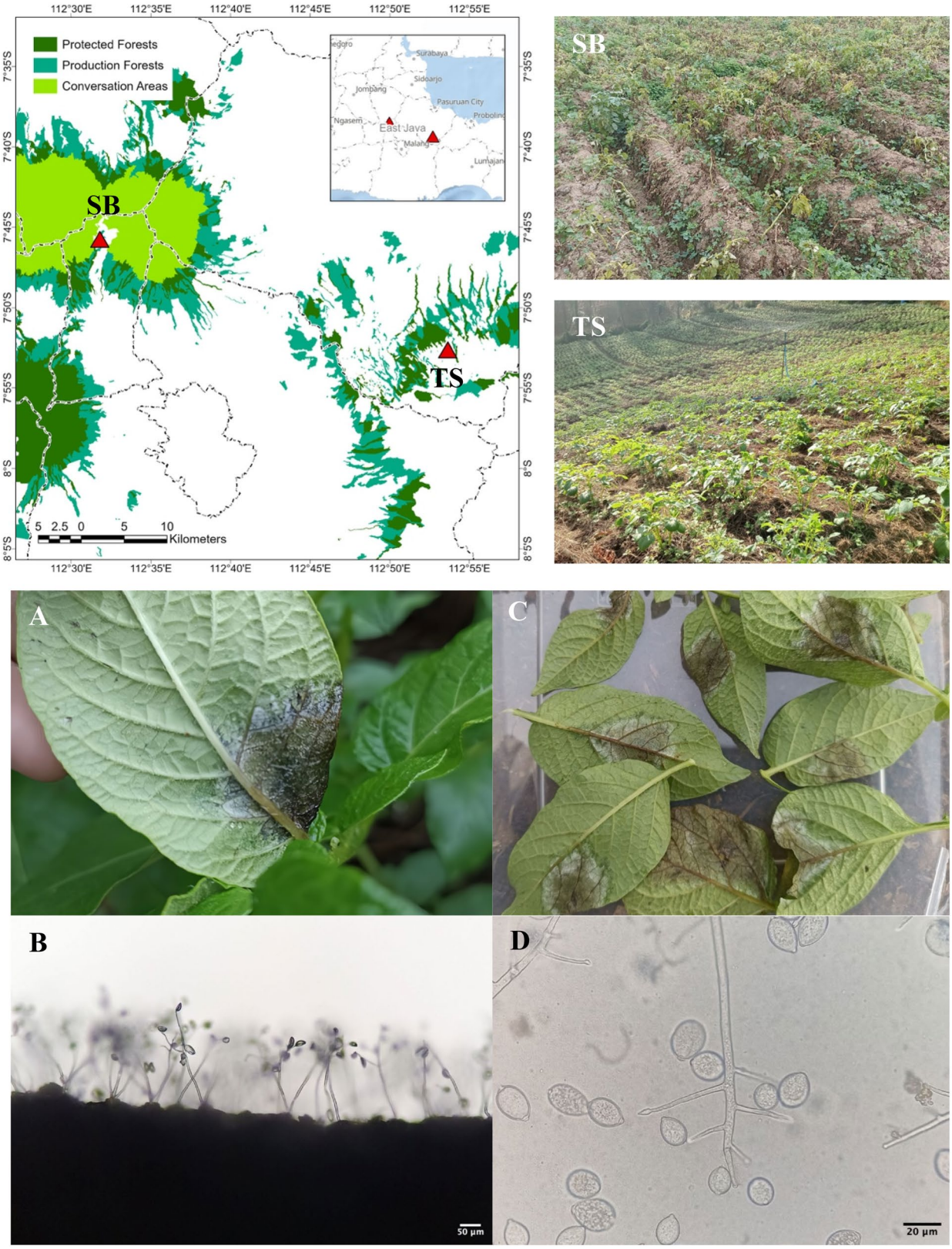

Figure 1. Sampling locations and symptomatic potato foliage caused by *Phytophthora infestans* in East Java. (A) Representative symptomatic leaflets in the field indicating the two sampled regions: the apical (leaf tip) region and the marginal (leaf edge) region. Field sources: Sumber Brantas (SB), Batu City and Tosari (TS), Pasuruan Regency. (B) Bright-field micrographs (dry-mount) of the abaxial surface from these regions at 10x, showing surface-borne sporulation along lesion margins (single arrowheads). (C) Higher-magnification view of the abaxial surface highlighting branched sporangiophores and sporangia. (D) Microscopic features caused by *Phytophthora infestans*, including dichotomously branched sporangiophores bearing ovoid to lemon-shaped sporangia (double arrowheads). Images were acquired using an Olympus BX41 microscope with an Olympus DP26 camera; only linear brightness/contrast adjustments were applied. Note: Panel letters (A–D) denote image type; TS and SB denote collection sites.

resolving key microscopic features consistent with *P. infestans*.

2.3. DNA extraction

Genomic DNA was extracted from symptomatic leaf tissue using the Plant Genomic DNA Mini Kit (Geneaid Biotech Ltd., Taipei, Taiwan). Approximately 50 mg of frozen tissue was ground in liquid nitrogen with a sterile mortar and pestle and transferred to microtubes. Extractions followed the manufacturer's protocol (tissue lysis, DNA binding, washing, elution). DNA purity and concentration were assessed using a NanoDrop spectrophotometer (Thermo Fisher Scientific, USA); A260/280 ratios were 1.8–2.0 and concentrations ranged from 20–80 ng/μL. DNA was stored at −20 °C until analysis.

2.4. ITS amplification (amplicon-based sequencing)

The fungal ITS region was amplified with universal primers ITS1-F and ITS4. Each 10 μL PCR contained 2 μL DNA template, 5 μL Taq PCR Master Mix (TIANGEN, Beijing, China), 1 μL of each primer (10 μM), and 1 μL nuclease-free water. Cycling conditions were: 95 °C for 3 min; 35 cycles of 95 °C for 30 s, 55 °C for 30 s, and 72 °C for 60 s; final extension at 72 °C for 5 min. PCR products were run on 1% agarose gels (75 V, 60 min), stained with ethidium bromide, and visualized under UV transillumination; a single band at ~400–500 bp was observed for samples, while the no-template control (NTC) showed no bands (Supplementary Figure S1), confirming amplicon integrity (no primer-dimers or nonspecific products). PCR products were purified (column-based cleanup) and quantified using the Qubit™ dsDNA HS Assay (Thermo Fisher Scientific), yielding 8.5–25 ng/μL (all ≥ 8.5 ng/μL) with A260/280 ≈ 1.8–2.0; libraries were prepared only for samples meeting these criteria.

2.5. Oxford nanopore sequencing and bioinformatics

ITS amplicon sequencing was performed using the Oxford Nanopore platform. For each location, the pooled composite DNA (from five symptomatic leaves) was prepared for library construction with Oxford Nanopore Technologies kits following the manufacturer's instructions. Sequencing was carried out with MinKNOW v22.05.7; raw signals were basecalled using Guppy v6.1.5 in high-accuracy (HAC) mode.

FASTQ files were evaluated using NanoPlot for read-length and quality distributions. Low-quality reads (Q score < 7 and length < 200 bp) were removed with NanoFilt prior to downstream analyses. Taxonomic classification was performed using Centrifuge against the NCBI ITS RefSeq targeted-loci database (downloaded from the NCBI Targeted Loci repository). Per-site feature/OTU tables were normalized to relative abundances to account for differences in sequencing depth. Community diversity summaries and graphics were produced in R v4.2.0; visualizations included Pavian and Krona Tools. We note that long ITS amplicons from Nanopore can improve taxonomic resolution for certain fungal groups; higher per-read error rates were mitigated *via* high-accuracy basecalling and quality control.

Replication note. Because sequencing was performed on one site-level composite per location (no molecular replicates), diversity results are presented descriptively; inferential statistics (e.g., PERMANOVA) were not performed on the sequencing dataset.

2.6. Heatmap visualization

Heatmap visualization was conducted in R (v4.2.0) using the pheatmap package (v1.0.12). The top 40 fungal genera were selected based on their total relative abundance across samples. Prior to visualization, relative abundance values were log-transformed ($\log_{10}$) to reduce the impact of extreme values and improve the interpretability of the heatmap. This normalization compressed the wide range of abundance values, allowing subtle variations among less abundant genera to become more distinguishable and resulting in a more balanced and informative visualization of community composition.

2.7. FTIR (fourier transform infrared) spectroscopy

Symptomatic leaf subsamples ($n = 3$ per sites) from the same sites were ground in liquid nitrogen to a fine powder. Infrared spectra were acquired using a Shimadzu IRSpirit FTIR spectrophotometer equipped with an ATR accessory. Samples were placed directly on the ATR crystal and compressed with a pressure arm to ensure optimal contact. Background spectra were collected prior to each run. Spectra were recorded over 4000–400 cm^{-1} at 4 cm^{-1} resolution with 32 scans per spectrum. Each site was represented by three biological replicates. Spectral preprocessing and peak assignment were conducted in Essential FTIR (Operant LLC, USA), including baseline correction, Savitzky–Golay smoothing, and

vector normalization. Additional visualization was performed with OriginPro 2022 (OriginLab Corporation, USA).

2.8. Principal component analysis (PCA) of FTIR spectra

Preprocessed FTIR spectra were normalized, mean-centered, and scaled prior to ordination. PCA was conducted in R v4.2.0 using FactoMineR and factoextra (PCA() and fviz_pca_ind()). Because ITS sequencing yielded one composite per site while FTIR had $n = 3$ replicates per site, paired FTIR–taxa correlations were not performed; FTIR results are presented exploratorily to visualize cross-site biochemical patterns.

3. Results

3.1. Site characteristics and agronomic context

Tosari District (Pasuruan Regency) and Sumber Brantas Village, Bumiaji District (Batu City) were selected as representative highland sites for potato plants showing late blight symptoms (Figure 1). In 2023, Tosari was the largest potato-producing area in Pasuruan (4,370 ha; 3,529 ha in 2019), whereas Sumber Brantas covered 481 ha [21]. Tosari lies at ~1,700 masl in the Tengger Mountains; Sumber Brantas is located at 1,400–1,700 masl. Farmers grew "Granola Kembang" in Tosari and "Granola Lembang" in Sumber Brantas.

Both regions practice monoculture potato cultivation, with notable differences in reported management. Farmers in Sumber Brantas frequently apply systemic fungicides (e.g., mancozeb, chlorothalonil, ametoctradin, dimethomorph), whereas farmers in Tosari report less intensive chemical use alongside plastic mulching and higher organic inputs (~20 t ha^{-1} vs. ~0.5 t ha^{-1}). Soils differ as Andisols (Sumber Brantas) versus Inceptisols (Tosari), and pH ranges overlapped (Sumber Brantas 4.0–5.5; Tosari 4.5–5.5). These environmental and management contexts are descriptive (non-experimental) and are considered when interpreting cross-site patterns (Table 1).

Table 1. Comparison of potato cultivation practices in Sumber Brantas and Tosari.

Parameter	Sumber Brantas	Tosari
Variety	Granola Lembang	Granola Kembang
Fungicide (Active Ingredient)	Mancozeb, chlorothalonil, ametoctradin, dimethomorph	Propineb, mancozeb, chlorothalonil
Use of Mulch	Not used	Plastic mulch
Organic Fertilizer	Manure 0.5 ton/ha	Manure 20 ton/ha
Chemical Fertilizer	ZA 250 kg/ha, NPK 250 kg/ha	Phonska 100 kg/ha
Soil pH	4-5.5	4.5-5.5
Soil type	Andisol	Inceptisol

3.2. ITS amplicon sequencing overview

PCR amplification of the fungal ITS region yielded clear ~400–500 bp products (Supplementary Figure S1). Oxford Nanopore ITS amplicon sequencing produced 66,160 quality-filtered reads for Tosari and 50,864 for Sumber Brantas. Krona visualizations indicated a higher proportion of unclassified reads in Tosari (28,123; 43%) than in Sumber Brantas (14,126; 28%) (Figure 2). We note that a larger "unclassified" fraction may reflect database coverage and read characteristics, and is not necessarily evidence of higher ecological complexity.

Because reads were derived from one site-level composite per location, sequencing-derived community summaries are descriptive. Per-site feature tables were normalized to relative abundances before summarization.

3.3. Cross-site community composition

At the phylum level, the Sumber Brantas composite was enriched in Mucoromycota, while the Tosari composite was enriched in Ascomycota (Figure 2). These phylum-level contrasts are coincident with differences in site, cultivar, soils, and reported management, and therefore are interpreted without causal attribution. Similar cross-site patterns have been noted in other crop systems where environmental and management variation is associated with shifts in dominant fungal taxa [22–30].

Richness estimators computed on the site-level composites suggested higher richness/evenness for Tosari than Sumber Brantas (Observed OTUs 312 vs. 183; Chao1 572.33 vs. 361.25; Shannon 2.40 vs. 1.18; Simpson 0.85 vs. 0.45) (Figures 3 and S2). Given the lack of molecular replication for sequencing, these indices are presented for baseline comparison only. Heatmap summaries (Figure 4a) indicated higher genus-level relative abundances in Tosari. A Venn diagram based on taxon assignments (Figure 4b) showed 312 and 183 assigned OTUs/taxa for Tosari and Sumber Brantas, respectively, with 117 shared. We avoid interpreting these counts as species numbers and treat them as assigned OTUs/taxa from the composite profiles. While causality cannot be inferred here, prior studies note that shifts toward Ascomycota- or Mucoromycota-dominated assemblages can co-occur with environmental and management differences, with potential implications for decomposition traits and stress tolerance [22–32].

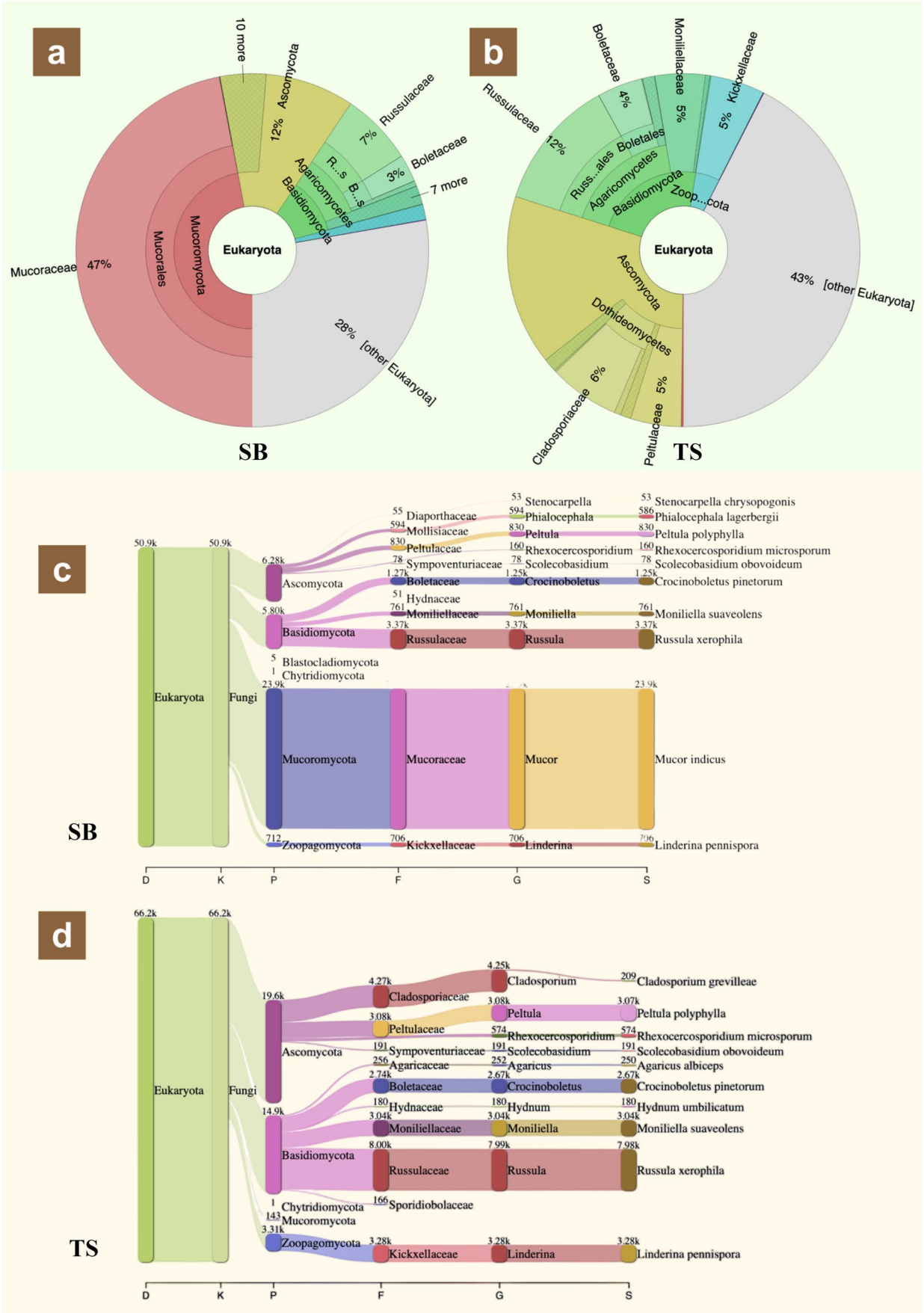

Figure 2. Comparison of phyllosphere fungal assignments using krona and Sankey diagrams. (a,c) Sumber Brantas (SB); (b,d) Tosari (TS). Exports shown at ≥300 dpi with enlarged labels for readability.

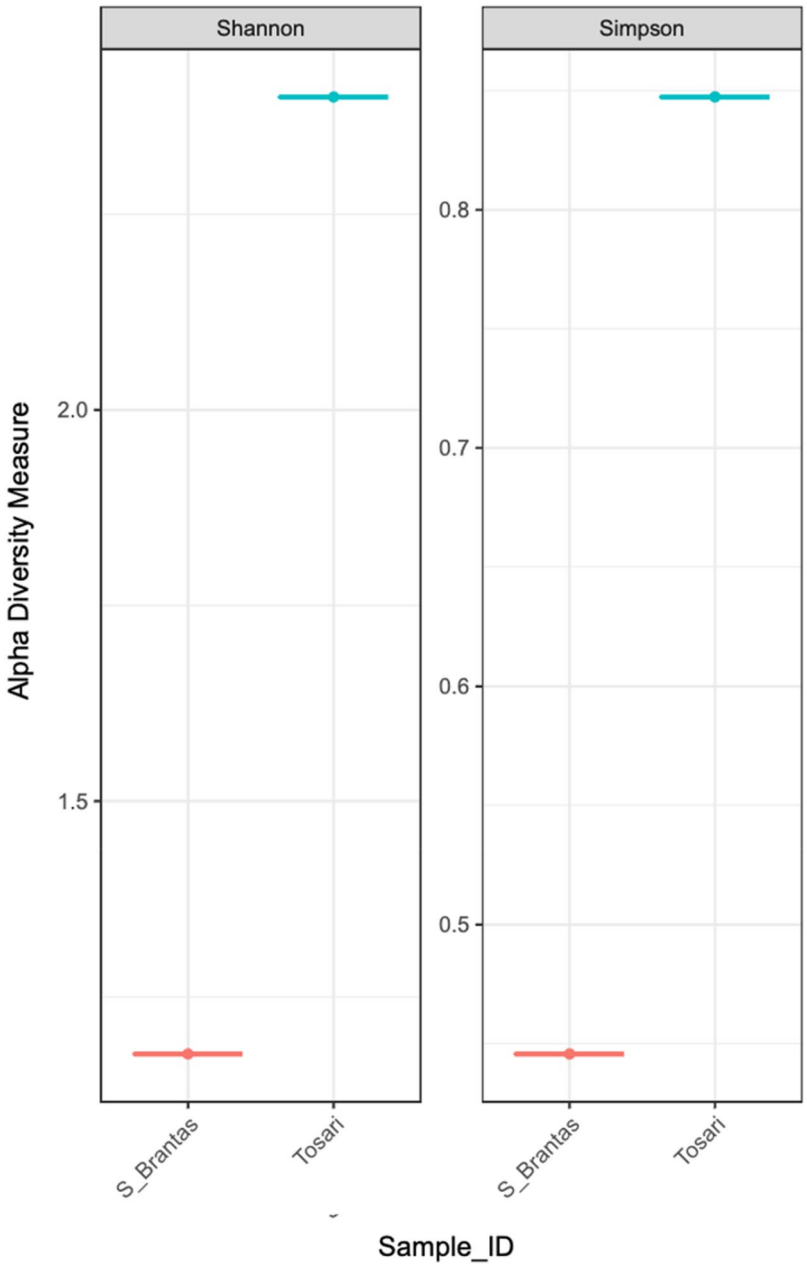

Figure 3. Alpha-diversity of phyllosphere fungal communities in Tosari and Sumber Brantas (descriptive, composite samples). Shannon (H′) and Simpson (1–D) indices computed from Oxford Nanopore ITS amplicon data after quality filtering (NanoFilt, Q < 7 and length < 200 bp removed) and normalization to relative abundances. Each value represents one site-level composite (five symptomatic leaves pooled per location).

3.4. FTIR spectral features

ATR-FTIR spectra from symptomatic leaves revealed site-differentiated biochemical signatures (Table 2). Each site was represented by three biological replicates. Replicates from Sumber Brantas showed consistent bands at 1641–1648 cm^{-1} (amide I), 2852–2853/2915–2919 cm^{-1} (aliphatic C–H stretching), and 3200–3400 cm^{-1} (O–H/N–H), indicative of proteinaceous, lipid-associated, and hydroxyl-bearing constituents (Figure 5) [18,19]. The amide I region is sensitive to protein secondary structure [33]. The broad O–H/N–H envelope (3200–3400 cm^{-1}) can overlap with phenolic signatures potentially associated with host stress responses to *Phytophthora infestans* [18–20,33,34]. Band assignments across amide, carbohydrate, and carbonyl regions are consistent with ATR-FTIR reports for plant tissues and microbial matrices [35–38], and the presence of polysaccharide/organic-acid signals in the 1200–900 cm^{-1} region is in line with literature on leaf and soil constituents [39].

In the fingerprint region (600–1800 cm^{-1}), Sumber Brantas showed peaks at 959 and 1009 cm^{-1} that were not evident in Tosari. These bands can involve polysaccharide C–O stretching and/or phosphodiester/CH out-of-plane vibrations. Both sites shared prominent bands at 1076–1094 cm^{-1} (C–C/C–O/PO_2^-), and amide III features near 1244–1246 and 1313–1318 cm^{-1}. A carbonyl band at 1726–1735 cm^{-1} is

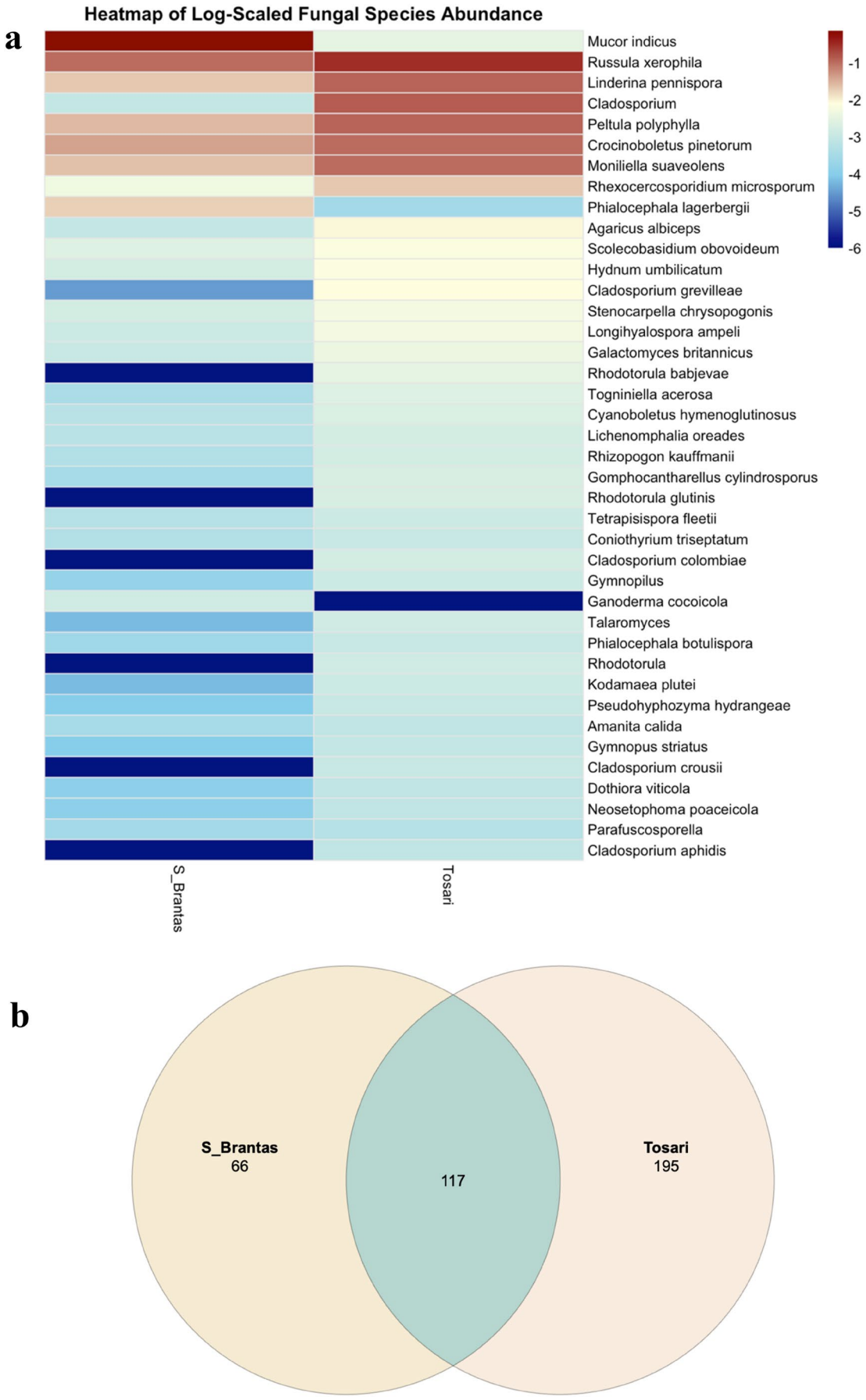

Figure 4. Heatmap of phyllosphere fungal abundance and shared taxa between Sumber Brantas and Tosari. (a) Heatmap showing relative abundance of fungal species (species names italicized) from Oxford Nanopore ITS amplicon reads classified with Centrifuge against the NCBI ITS RefSeq targeted-loci database. Columns correspond to site-level composites (Sumber Brantas; Tosari). The color scale indicates read abundance (log-like steps as displayed: ~1, 16, 256, 4096). (b) Venn diagram indicating shared and unique OTUs/taxa between the two site-level composites.

Table 2. FTIR spectral peaks and functional group assignment.

Wavenumber (cm^{-1})	Functional group/vibration	Possible compound class	Biological interpretation	Citation
511 (Tosari)	P–O bending/S–S stretching	Phosphate minerals, disulfide bonds (proteins)	May indicate inorganic phosphate residues or structural disulfide bonds in proteins	
536 (Sumber Brantas)	PO_4^{3-} bending (symmetric)	Phosphates, phospholipids, nucleic acids	Suggests phosphate accumulation, possibly microbial or plant-derived	
959 (Sumber Brantas)	C–O stretching/CH out-of-plane	Polysaccharides, nucleic acids	Likely microbial metabolites or carbohydrate/nucleic acid residues	
1009 (Sumber Brantas)	C–O stretching, CH out-of-plane	Carbohydrates, nucleic acids	Stress-induced carbohydrate signatures or DNA/RNA-related bands	
1076–1094	C–O, C–C stretching; PO_2^- symmetric	Polysaccharides, DNA/RNA	Structural polysaccharides, microbial cell wall, or nucleic acids	[19]
1244–1246	Amide III (C–N stretch + N–H bend); PO_2^- asymmetric	Proteins, nucleic acids	Protein secondary structure, possible overlap with DNA/RNA	[19,31,32]
1313–1318	Amide III	Proteins	Proteinaceous compounds (peptides, enzymes)	[32]
1410 (Sumber Brantas)	COO^- symmetric stretch	Organic acids, pectin	Carboxylate-rich metabolites, linked to stress metabolism	
1547 (Tosari)	Amide II (N–H bend + C–N stretch)	Proteins, peptides	Protein structures, stress-related conformations	[24]
1641–1648	Amide I (C = O stretching)	Proteins	Protein backbone, α-helix/β-sheet balance	[25]
1726–1735	C = O ester stretching	Lipids, pectin, phospholipids	Membrane lipids, esterified polysaccharides	[20,32]
2852–2853	CH_2 symmetric stretch	Lipids (fatty acids, phospholipids)	Lipid chains, cuticular waxes	[18]
2915–2919	CH_2 asymmetric stretch	Lipids (fatty acids, phospholipids)	Membrane lipid content	[32,34,40]
3200–3400	O–H/N–H stretching	Water, hydroxyls, amines	Bound water, phenolics, protein hydrogen bonding	[41,42]

consistent with esters (e.g., lipids/phospholipids) [18,19,34,40]. Overall intensity differences across amide and O–H/N–H regions suggest distinct leaf biochemical states between sites; however, we do not infer that these FTIR differences are caused by microbiome composition or management alone, as they most likely reflect host physiological responses to late blight infection.

3.5. PCA of FTIR spectra

PCA of preprocessed FTIR spectra separated sites along PC1–PC2 (e.g., 48.1% and 31.7% of variance, respectively) (Figure 6). Sumber Brantas replicates clustered tightly (positive PC1), while Tosari occupied negative PC1 space. Loadings highlighted contributions from amide I (1641–1648 cm^{-1}), O–H/N–H (3200–3400 cm^{-1}), and 959/1009 cm^{-1} to Sumber Brantas separation, and contributions from 1076–1094 cm^{-1} (carbohydrate-associated) and 2852–2919 cm^{-1} (aliphatic C–H) toward Tosari. These ordinations visualize cross-site biochemical differences and are interpreted exploratorily (no paired FTIR–taxa correlations were performed due to sequencing composites). These findings are consistent with prior reports demonstrating the utility of FTIR–PCA for discriminating sample groups based on biochemical signatures under varying conditions [41,42].

4. Discussion

Cross-site contrasts in the composite ITS profiles (Ascomycota-enriched in Tosari; Mucoromycota-enriched in Sumber Brantas) and FTIR spectra (amide/O–H/N–H prominence and 959/1009 cm^{-1} features in Sumber Brantas) indicate differences in leaf-associated fungal assemblages and biochemical states under late blight pressure. These biochemical differences captured by FTIR are likely dominated by host metabolic responses to infection rather than by microbial composition per se. Because the study used one sequencing composite per site and involved different cultivars, soils, and management contexts, we interpret these patterns as associations rather than causal effects. Mechanistically, members of Ascomycota encompass diverse endophytes and saprotrophs with enzyme portfolios linked to leaf-surface resource use, whereas Mucoromycota include taxa reported from stress-affected or disturbance-prone niches [31,32]. Such patterns in our composites are consistent with context-dependent assembly rather than single-factor control.

The descriptive richness/evenness indices for the composites were higher for Tosari than Sumber Brantas, consistent with literature showing that frequent chemical inputs can coincide with lower fungal diversity, while organic amendments/mulching can coincide with richer microbial assemblages [43–50].

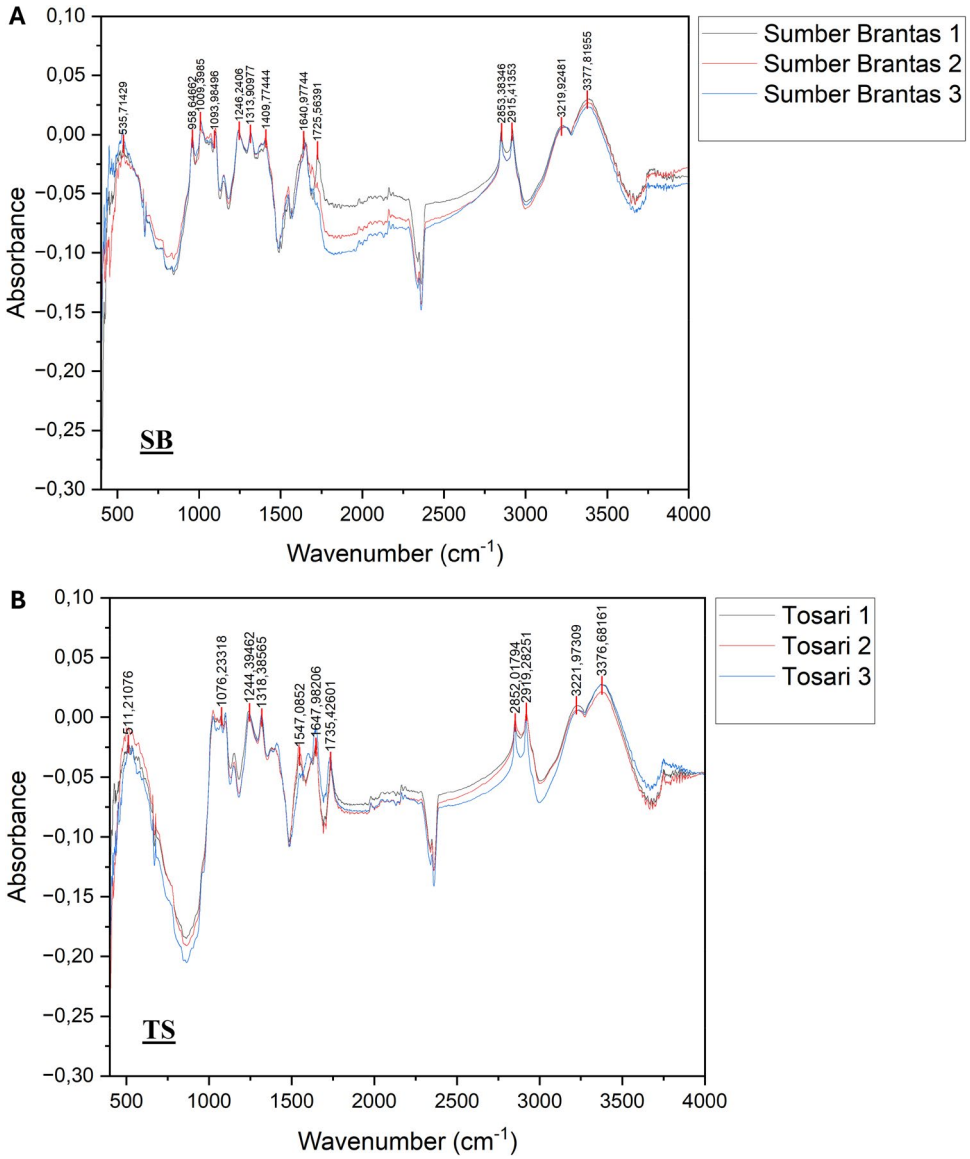

Figure 5. FTIR spectra are interpreted as exploratory biochemical profiles illustrating cross-site biochemical variation. Panels: (a) Sumber Brantas (three replicates); (b) Tosari (three replicates).

These descriptive observations also align with studies reporting that fungicide applications can affect non-target fungal communities in the phyllosphere and soil and alter overall community structure [24–30]. In parallel, efficacy and usage patterns of specific active ingredients (e.g., ametoctradin–dimethomorph combinations) have been documented in other pathosystems, underscoring the need to balance disease control with potential community-wide effects [51]. Similarly, FTIR band patterns (amide I, O–H/N–H, carbonyl, and fingerprint peaks) reflect leaf biochemical differences that may involve host responses to *Phytophthora infestans*, microbial metabolites, and/or environmental inputs [18–20,33,34,40]. Without paired molecular replicates, we do not claim direct correspondence between specific taxa and FTIR bands.

Additionally, several studies report that specific cultivation/amelioration practices can shape phyllosphere communities *via* changes in microhabitats and resource availability [22,23]. More broadly, these observations align with the pivotal roles of phyllosphere microorganisms at the plant–atmosphere interface and their interactions with other microbial guilds, which can shape host physiology and stress responses [52,53]. Collectively, the integrative (ITS–FTIR) readouts provide a baseline for designing controlled follow-ups (e.g., replicate ITS per plant, within-site gradients of fungicide/organic inputs, and healthy-leaf controls) and for testing targeted hypotheses about management–microbiome–biochemistry linkages. Such designs would enable statistical inference (e.g., PERMANOVA with dispersion checks) and taxon–band association testing with appropriate correction. Future studies incorporating biological replication for both ITS and FTIR datasets will be required to statistically assess cross-modality associations.

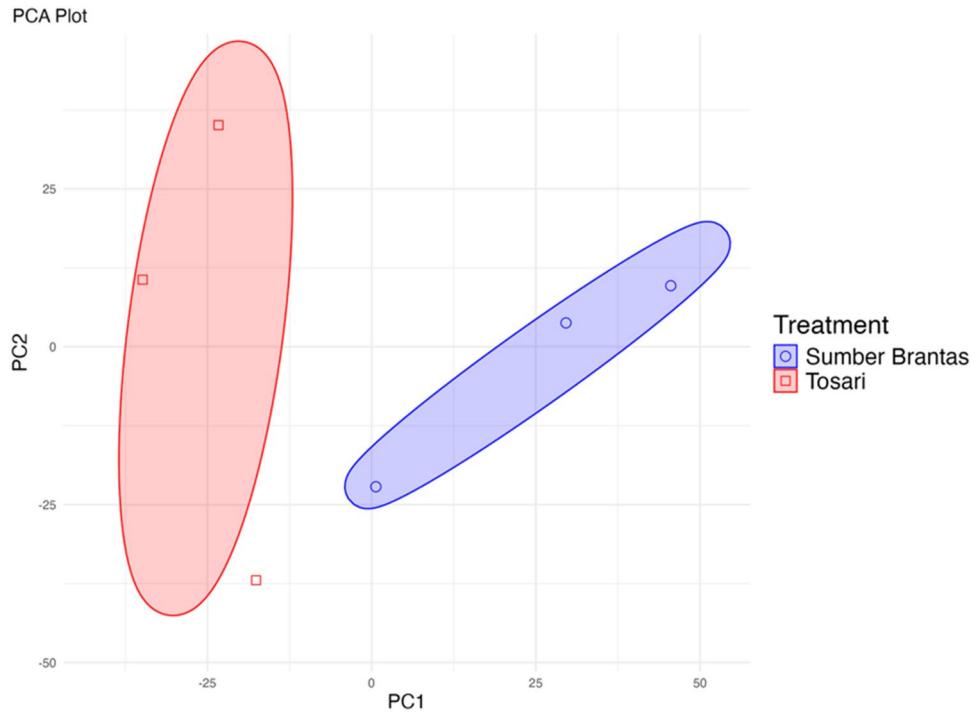

Figure 6. Principal component analysis (PCA) of preprocessed FTIR spectral data from symptomatic potato leaves collected at Sumber Brantas and Tosari. Each point represents one biological replicate ($n = 3$ per site). PC1 (48.1%) and PC2 (31.7%) explain most of the variance, with Sumber Brantas samples clustering along positive PC1 and Tosari along negative PC1. The PCA visualizes site-level biochemical differentiation between the two highland cultivation contexts.

Acknowledgments

The authors thank the Department of Plant Pest and Disease, Faculty of Agriculture, Universitas Brawijaya, Malang, Indonesia for the Laboratory Facilities provided during this research.

Disclosure statement

No potential conflict of interest was reported by the author(s).

Use of Generative AI

ChatGPT (OpenAI, GPT-5, 2025) was used solely to assist with language polishing and improving readability in parts of the manuscript (e.g., Introduction and Discussion). All content was critically reviewed, edited, and validated by the authors to ensure accuracy, originality, and compliance with scientific and ethical standards.

Funding

This work was supported by Professor Grants of Universitas Brawijaya 2023 [number 4744.24/UN10.F04/PN/2023].

ORCID

Abdul Latief Abadi http://orcid.org/0000-0001-6076-8028
Muhammad Akhid Syib'li http://orcid.org/0000-0003-2617-137X
Irisa Trianti http://orcid.org/0000-0003-4431-758X
Valia Istifada http://orcid.org/0009-0001-4913-6027
Sholikah Widyanitta Rachmawati http://orcid.org/0009-0004-0284-1601
Bayu Aji Pamungkas http://orcid.org/0009-0006-7532-0852

Data availability statement

The authors confirm that the data supporting the findings of this study are available within the article and its supplementary materials.

References

[1] Sivakumar N, Sathishkumar R, Selvakumar G, et al. Phyllospheric microbiomes: diversity, ecological significance, and biotechnological applications. Plant Microbiomes Sustain Agric. 2020;25:113–172. doi: 10.1007/978-3-030-38453-1_5.
[2] Insani N, Ridhoi R, Hidajat HG, et al. Pro-environmental tourism: lessons learned from adventure, wellness and eco-tourism in Padusan Village, Mojokerto, East Java. IOP Conf. Ser. Earth Environ. Sci. 2024;1313(1):012043. doi: 10.1088/1755-1315/1313/1/012043.
[3] Fry WE, Birch PRJ, Judelson HS, et al. Five reasons to consider *Phytophthora infestans* a reemerging pathogen. Phytopathology. 2015;105(7):966–981. doi: 10.1094/PHYTO-01-15-0005-FI.
[4] Haverkort AJ, Boonekamp PM, Hutten R, et al. Societal costs of late blight in potato and prospects of durable resistance through cisgenic modification. Potato Res. 2008;51(1):47–57. doi: 10.1007/s11540-008-9089-y.
[5] Naveed K, Khan SA, Rajput NA, et al. Population structure of *Phytophthora infestans* on worldwide scale: a review. Pak J Phytopathol. 2017;29(2):281–288. doi: 10.33866/phytopathol.029.02.0402.
[6] Rakotonindraina T, Chauvin JÉ, Pellé R, et al. Modeling of yield losses caused by potato late blight on eight cultivars with different levels of resistance

to *Phytophthora infestans*. Plant Dis. 2012;96(7):935–942. doi: 10.1094/PDIS-09-11-0752.
[7] Massi F, Torriani SFF, Borghi L, et al. Fungicide resistance evolution and detection in plant pathogens: *Plasmopara viticola* as a case study. Microorganisms. 2021;9(1):119. doi: 10.3390/microorganisms9010119.
[8] Meyer C, Jeanbille M, Breuil MC, et al. Soil microbial community fragmentation reveals indirect effects of fungicide exposure mediated by biotic interactions between microorganisms. J Hazard Mater. 2024;470:134231. doi: 10.1016/j.jhazmat.2024.134231.
[9] Bashir I, War AF, Rafiq I, et al. Phyllosphere microbiome: diversity and functions. Microbiol Res. 2022;254:126888. doi: 10.1016/j.micres.2021.126888.
[10] Ren P, Sun A, Jiao X, et al. National-scale investigation reveals the dominant role of phyllosphere fungal pathogens in sorghum yield loss. Environ Int. 2024;185:108511. doi: 10.1016/j.envint.2024.108511.
[11] Schmidt JE, Puig AS, DuVal AE, et al. Phyllosphere microbial diversity and specific taxa mediate within-cultivar resistance to *Phytophthora palmivora* in cacao. mSphere. 2023;8(5):e00013-23. doi: 10.1128/msphere.00013-23.
[12] Mukesh S, Mohammad S, Sonika P, et al. *Trichoderma*: a scientific approach against soil borne pathogens. Afr. J. Microbiol. Res. 2015;9(50):2377–2384. doi: 10.5897/AJMR2015.7788.
[13] Sumbula V, Kurian PS, Girija D, et al. Impact of foliar application of fungicides on tomato leaf fungal community structure revealed by metagenomic analysis. Folia Microbiol. 2022;67(1):103–108. doi: 10.1007/s12223-021-00920-x.
[14] Lloyd AW, Percival D, Yurgel SN. Effect of fungicide application on lowbush blueberries soil microbiome. Microorganisms. 2021;9(7):1366. doi: 10.3390/microorganisms9071366.
[15] Iqbal R, Raza MAS, Valipour M, et al. Potential agricultural and environmental benefits of mulches—a review. Bull Natl Res Cent. 2020;44(1):75. doi: 10.1186/s42269-020-00290-3.
[16] Chalker-Scott L. Impact of mulches on landscape plants and the environment—a review. J Environ Hortic. 2007;25(4):239–249. doi: 10.24266/0738-2898-25.4.239.
[17] Arif M. Unraveling the diversity and spatial distribution of soil-borne fungal mycobiomes with response to environmental parameters, cropping schemes and cropping seasons. J Agric Biotechnol. 2024;5(1):19–32. doi: 10.58728/joinabt.1486927.
[18] Topală CM, Rusea I. Analysis of leaves using FTIR spectroscopy and principal component analysis discrimination of different plant samples. IOP Conf Ser Earth Environ Sci. 2018;7:286–291. doi: 10.1088/1755-1315/1313/1/012043.
[19] Munteanu AL, Vijan LE, Topală CM, et al. Influence of the phytosanitary status, cultivar, and harvest time on the phenolic, chlorophyll, and alkaloid content of *Rosa* sp. leaves. Horticulturae. 2023;9(11):1169. doi: 10.3390/horticulturae9111169.
[20] Nuzzo A, Buurman P, Cozzolino V, et al. Infrared spectra of soil organic matter under a primary vegetation sequence. Chem. Biol. Technol. Agric. 2020;7(1):12. doi: 10.1186/s40538-019-0172-1.
[21] Statistics Indonesia. Statistics of seasonal vegetables and fruits in Indonesia. 2023. Available from: https://www.bps.go.id/en/publication/2017/10/02/9d10a13049cee1ce8aad9768/statistics-of-seasonal-vegetable-and-fruit-plants-in-indonesia-2016.html
[22] Ding H, Ali A, Cheng Z. Dynamics of a soil fungal community in a three-year green garlic/cucumber crop rotation system in Northwest China. Sustainability. 2018;10(5):1391. doi: 10.3390/su10051391.
[23] Wu PH, Chang HX, Shen YM. Effects of synthetic and environmentally friendly fungicides on powdery mildew management and the phyllosphere microbiome of cucumber. PLoS One. 2023;18(3):e0282385. doi: 10.1371/journal.pone.0282385.
[24] Karlsson I, Friberg H, Steinberg C, et al. Fungicide effects on fungal community composition in the wheat phyllosphere. PLoS One. 2014;9(11):e111786. doi: 10.1371/journal.pone.0111786.
[25] Sapkota R, Knorr K, Jørgensen LN, et al. Host genotype is an important determinant of the cereal phyllosphere mycobiome. New Phytol. 2015;207(4):1134–1144. doi: 10.1111/nph.13418.
[26] Noel ZA, Longley R, Benucci GMN, et al. Non-target impacts of fungicide disturbance on phyllosphere yeasts in conventional and no-till management. ISME Commun. 2022;2(1):103. doi: 10.1038/s43705-022-00103-w.
[27] Ben Naim Y, Cohen Y. Replacing mancozeb with alternative fungicides for the control of late blight in potato. J Fungi. 2023;9(11):1046. doi: 10.3390/jof9111046.
[28] Huang Z, Wang P, Pu Z, et al. Effects of mancozeb on citrus rhizosphere bacterial community. Microb Pathog. 2021;154:104845. doi: 10.1016/j.micpath.2021.104845.
[29] Baćmaga M, Wyszkowska J, Kucharski J. The influence of chlorothalonil on the activity of soil microorganisms and enzymes. Ecotoxicology. 2018;27(9):1188–1202. doi: 10.1007/s10646-018-1968-7.
[30] Jiang J, Yang Y, Wang L, et al. Effects of chlorothalonil application on the physio-biochemical properties and microbial community of a yellow–brown loam soil. Agriculture. 2022;12(5):608. doi: 10.3390/agriculture12050608.
[31] Bonfante P, Venice F. Mucoromycota: going to the roots of plant-interacting fungi. Fungal Biol Rev. 2020;34(2):100–113. doi: 10.1016/j.fbr.2019.12.003.
[32] Challacombe JF, Hesse CN, Bramer LM, et al. Genomes and secretomes of *Ascomycota* fungi reveal diverse functions in plant biomass decomposition and pathogenesis. BMC Genomics. 2019;20(1):976. doi: 10.1186/s12864-019-6358-x.
[33] Movasaghi Z, Rehman S, Rehman IU. Fourier transform infrared (FTIR) spectroscopy of biological tissues. Appl Spectrosc Rev. 2008;43(2):134–179. doi: 10.1080/05704920701829043.
[34] Wu X, Hao Y, Riaz M, et al. Changes in leaf structure and chemical compositions investigated by FTIR are correlated with different low potassium adaptation of two cotton genotypes. Agronomy. 2020;10(4):479. doi: 10.3390/agronomy10040556.
[35] Kamnev AA, Dyatlova YA, Kenzhegulov OA, et al. Fourier Transform Infrared (FTIR) spectroscopic analyses of microbiological samples and biogenic se-

lenium nanoparticles of microbial origin: sample preparation effects. Molecules. 2021;26(4):1146. doi: 10.3390/molecules26041146.

[36] Topala CM, Paunescu A, Soare LC. ATR-FTIR spectral analysis of ferns using as fingerprint for identification of fern species. Rev. Chim. 2019;70(3):875–880. doi: 10.37358/RC.19.3.7024.

[37] Meena KK, Sorty AM, Bitla UM, et al. Abiotic stress responses and microbe-mediated mitigation in plants: the omics strategies. Front Plant Sci. 2017;8:172. doi: 10.3389/fpls.2017.01772.

[38] Straková P, Larmola T, Andrés J, et al. Quantification of plant root species composition in peatlands using FTIR spectroscopy. Front Plant Sci. 2020;11:597. doi: 10.3389/fpls.2020.00597.

[39] Vranova V, Rejsek K, Formanek P. Aliphatic, cyclic, and aromatic organic acids, vitamins, and carbohydrates in soil: a review. ScientificWorldJournal. 2013; 2013(1):524239. doi: 10.1155/2013/524239.

[40] Li X, Zhang L, Zhang S, et al. Detection of Verticillium infection in cotton leaves using ATR-FTIR spectroscopy coupled with machine learning algorithms. Spectrochim Acta A Mol Biomol Spectrosc. 2025; 325:125127. doi: 10.1016/j.saa.2024.125127.

[41] Zhou H, Fu H, Wu X, et al. Discrimination of tea varieties based on FTIR spectroscopy and an adaptive improved possibilistic c-means clustering. J. Food Process. Preserv. 2020;44(10):e14795. doi: 10.1111/jfpp.14795.

[42] Ng JXY, Tan NSL, Chung WH, et al. A study on the surface responses and degradation mechanisms of epoxy-amine coating subjected to UV accelerated weathering and hygrothermal ageing using ToF-SIMS and FTIR analysis. Polym Degrad Stab. 2024;228: 110930. doi: 10.1016/j.polymdegradstab.2024.110930.

[43] Kozak ÖS, Erkiliç A. Effects of some fungicides and foliar fertilizers on epiphytic fungal and yeast population of citrus leaves. Süleyman Demirel Üniversitesi Fen Bilimleri Enstitüsü Dergisi. 2018;22(2):429–435. doi: 10.19113/sdufbed.65085.

[44] Baćmaga M, Wyszkowska J, Kucharski J. The effect of the Falcon 460 EC fungicide on soil microbial communities, enzyme activities and plant growth. Ecotoxicology. 2016;25(8):1575–1587. doi: 10.1007/s10646-016-1713-z.

[45] Zhalnina K, Dias R, de Quadros PD, et al. Soil pH determines microbial diversity and composition in the park grass experiment. Microb Ecol. 2015;69(2): 395–406. doi: 10.1007/s00248-014-0530-2.

[46] Zhou H, Zhang D, Jiang Z, et al. Changes in the soil microbial communities of alpine steppe at Qinghai-Tibetan Plateau under different degradation levels. Sci Total Environ. 2019;651(2):2281–2291. doi: 10.1016/j.scitotenv.2018.09.336.

[47] Zhou J, Jiang X, Zhou B, et al. Thirty four years of nitrogen fertilization decreases fungal diversity and alters fungal community composition in black soil in northeast China. Soil Biol Biochem. 2016;95:135–143. doi: 10.1016/j.soilbio.2015.12.012.

[48] Yao Q, Liu J, Yu Z, et al. Three years of biochar amendment alters soil physiochemical properties and fungal community composition in a black soil of northeast China. Soil Biol Biochem. 2017;110:56–67. doi: 10.1016/j.soilbio.2017.03.005.

[49] Naresh P, Singh I. Organic mulching in regenerative agriculture enhances saprotrophs and concomitantly reduces pathogenic fungal genera. J Sustain Agric Environ. 2025;4(2):1–15. doi: 10.1002/sae2.70066.

[50] Wei B, Bi J, Qian X, et al. Organic manure amendment fortifies soil health by enriching beneficial metabolites and microorganisms and suppressing plant pathogens. Agronomy. 2025;15(2):429. doi: 10.3390/agronomy15020496.

[51] Ramallo AC, Olmedo GM, Ramallo J, et al. Effectiveness of an ametoctradin-dimethomorph formulation to control brown rot on postharvest lemons. Sci Hortic. 2019;246:574–577. doi: 10.1016/j.scienta.2018.11.035.

[52] Bringel F, Couée I. Pivotal roles of phyllosphere microorganisms at the interface between plant functioning and atmospheric trace gas dynamics. Front Microbiol. 2015;6:486. doi: 10.3389/fmicb.2015.00486.

[53] Singh M, Vyas D, Singh PK. Interaction of soil microbes with mycorrhizal fungi in tomato. Arch Phytopathol Plant Prot. 2014;47(6):737–743. doi: 10.1080/03235408.2013.820389.